

Importance of Magnetism in Phase Stability, Equations of State, and Elasticity

R. E. COHEN, S. GRAMSCH, S. MUKHERJEE

Geophysical Laboratory, Carnegie Institution of Washington, Washington, D.C. 20015

G. STEINLE-NEUMANN, and L. STIXRUDE

Department of Geological Sciences, University of Michigan, Ann Arbor, MI 48109

Summary. — The effects of magnetism on high pressure properties of transition metals and transition metal compounds can be quite important. In the case of Fe, magnetism is responsible for stability of the body-centered cubic (bcc) phase at ambient conditions, and the large thermal expansivity in face-centered cubic (fcc) iron, and also has large effects on the equation of state and elasticity of hexagonal close-packed (hcp) iron. We find evidence for non-collinear magnetism in hcp iron below about 50 GPa. In transition metal oxides, local magnetic moments are responsible for their insulating behavior. LDA+U results are presented for CoO and FeO, and predictions are made for high pressure metallization. The inclusion of a local Coulomb repulsion, U , greatly inhibits the high-spin low-spin transitions found with conventional exchange-correlation functionals (i.e. generalized gradient corrections, GGA). We discuss theory and computations for the effects of magnetism on high pressure cohesive properties.

1. – Magnetism

One might think that one needs to be concerned with magnetism only if one is interested in magnetic properties of materials. This is not the case! Rather the stable crystal structure can depend on properly taking into account magnetism, which can strongly affect phase stability, lattice distortions, elasticity, equations of state, and vibrational frequencies. Furthermore, magnetism can be important in materials containing transition metal ions even when the magnetic moments are not ordered. The distinction between “non-magnetic” materials and disordered, paramagnetic, materials is crucial.

Magnetism in crystals comes about because electrons have a quantity called spin, which is a vector quantity that behaves like quantum angular momentum. Electrons also have orbital angular momentum, which can lead to orbital magnetic moments. In heavy transition metal ions with partially occupied f-electron shells, such as rare earths or lanthanides, these orbital moments can be very important.

Here we will concentrate on d-electron systems, but there is much complex and fascinating physics in the f-electron systems. In the f-electron systems, the f-electrons tend to form very localized, strong magnetic moments on each atom. The localized f-electrons then interact with delocalized band-like states, and this interaction can lead to interesting phase transitions with pressure, for example in Ce [1]. Electronic d-states tend to be more delocalized than f-states, though localization is important, as we will discuss below.

The fact that electronic wave functions are antisymmetric with respect to exchanging two electrons leads to the Pauli exclusion principle, without which electrons would all fall into the nucleus, and there would be no atoms. The exclusion principle states that two electrons cannot be in the same state. If electrons did not have spin the universe would be a very different place, since only one electron could then be put into each band. Since electrons do have spin, it is possible for two electrons to occupy the same state, with one electron having the opposite spin of the other. In many atoms, molecules, crystals, and liquids, the electrons are paired up, with each member of the pair having the same probability distribution in space, but with opposite spins. These spin states are conventionally called “spin-up” and “spin-down”, though there is nothing “up” or “down” about them except the way they might be drawn. Note that one must be careful to understand that the concept of electron pairing in states is a rather loose way of talking. In reality electrons are indistinguishable from each other, and one should talk about the quantum states being paired, rather than particular electrons.

Electrons have an effective interaction that is different depending on whether they have the same spin or not. Since electrons with opposite spin can occupy the same space, they have a higher potential energy of interaction on average. Thus all else being equal, electrons would want to have the same spin in order to lower the system’s potential energy. A system with electrons that have the same spin direction is a ferromagnet. There is no free lunch, though. The cost of lowering the potential energy by lining up the spins is to raise the system’s kinetic energy, since higher states must be occupied instead of the lower energy paired states. Thus there is competition between electronic potential energy which favors magnetism, and the electronic kinetic energy, which favors

a non-magnetic electronic structure. As pressure is increased, electrons are pushed close together, and the relative potential energy change between paired and unpaired electrons becomes less important; bands become wider, making the kinetic energy cost smaller, so that in general materials become non-magnetic with increasing pressure. The total energy change between the magnetic and non-magnetic system in the simple picture presented so far is known as the exchange energy.

As temperature is raised from low temperatures, the magnetic moment directions on each atom will fluctuate more and more, and at some critical temperature, called the Curie temperature, or T_C in ferromagnets, the moments will disorder. In general, there are still magnetic moments on the ions above T_C , they are just disordered in direction.

Antiferromagnets have moments of opposite direction on alternating sites. It is the different hybridization of electronic states that leads to antiferromagnetic rather than ferromagnetic order, so that the kinetic energy is lowered. This is sensitive to pressure, so some ferromagnets become antiferromagnetic with increasing pressure, as in fcc iron.

In some cases the lowest free energy state has non-collinear spins. This can arise from “frustration,” which is the situation where it is impossible to tile a lattice with a perfect antiferromagnetic pattern, with every atom having only neighbors with the opposite pointing spin. Examples are fcc and hcp structures, as will be discussed below. Such effects can be very important to material properties, and are responsible for the anti-Invar effect (high thermal expansivity) in fcc Fe, for example.

This is not meant as a comprehensive review, but rather as lecture notes, and an introduction of this complex field to the student. Examples are mainly chosen from our own theoretical work, or from published experiments.

1.1. *Itinerant magnetism.* – There are two endmember models for understanding antiferromagnetism. In the band, or Slater, picture [2], it is the different exchange interactions between like- and unlike-spin electrons, combined with the kinetic energy of the resulting different band states that leads to the stability of antiferromagnetic, rather than ferromagnetic or non-magnetic states. Antiferromagnetism is a zone-boundary instability that leads to a doubling of the unit cell, giving folding of the electronic states. These states then hybridize differently through the exchange potential than they would have in the ferromagnetic case.

The Stoner model demonstrates the band picture of magnetism, and though a simple model, turns out to be predictive. In the Stoner model, the magnetization energy ΔE is

$$(1) \quad \Delta E = \frac{-IM^2}{4} + \frac{M^2}{4N(0)}$$

where M is the magnetic moment or magnetization, the Stoner Integral I is an atomic property, $N(0)$ is the density of states at the Fermi level (or top of the valence band). The first-term on the right hand side is the magnetic energy and the second is the change in the band energy with magnetic moment. Minimization of ΔE gives the Stoner criterion:

$$(2) \quad IN(0) > 1$$

for a magnetic state to be stable. In the more sophisticated extended Stoner model, the average density of states,

$$(3) \quad \tilde{N}(M) = M/\delta\epsilon,$$

is used, where $\delta\epsilon$ is the spin (exchange) splitting, and

$$(4) \quad \tilde{N}(0) = N(0) = \partial M/\partial\delta\epsilon.$$

The instability criterion is $I\tilde{N}(M) > 1$. As pressure is increased the effective density of states generally decreases, and magnetism will decrease and disappear with increasing pressure.

Figure 1 shows Stoner diagrams for CoO, hypothetical FeSiO₃ in the cubic perovskite structure, and FeO in the NiAs structure. With increasing pressure the effective density of states drops, and the stable magnetic structure becomes low-spin due to this effect.

The Stoner model is a rigid band model. One can go beyond this with a tight-binding model, which is intermediate in accuracy and speed between self-consistent methods and the Stoner model. In a tight-binding model, the Hamiltonian and overlap matrix elements are parametrized. A first-principles tight-binding model has been developed that is fit to first-principles total energies and band eigenvalues [3]. One can obtain a magnetic model by doubling the size of the Hamiltonian, and adding or subtracting $IM^2/2$ to the spin-up and spin-down diagonal Hamiltonian elements, giving Hamiltonian H_{collin} . Actually in the collinear case one can diagonalize the spin-up and spin-down block separately. Then the total energy is given by

$$(5) \quad E = E_{bs} + \sum \frac{Im_i^2}{4}$$

where E_{bs} is the band structure energy (sum of the occupied band eigenvalues) and m_i is the moment on each site. A non-collinear model can be obtained by rotating the Hamiltonian matrix. In the non-collinear case, the eigenproblem does not factorize and spin-up and spin-down states hybridize. The final Hamiltonian is then given by

$$(6) \quad H_{non-collin} = R^{-1}H_{collin}R$$

where R is the site-dependent rotation matrix. The moments obtained by occupying states up to the Fermi level do not necessarily equal the input moments, so self-consistency cycles are performed until the output and input moments are equal. Thus the output is the moment on each site and the total energy. Details will be given elsewhere. See also ref. [41]. We discuss results for Fe from this model below.

1.2. Mott insulators. – Predicting properties of transition metal-bearing oxides is a severe problem in modern band theory, although qualitative understanding of the behavior of transition metal oxides has been developed [5, 6]. Examples of problem compounds are CoO and FeO; conventional band theory (the local density approximation,

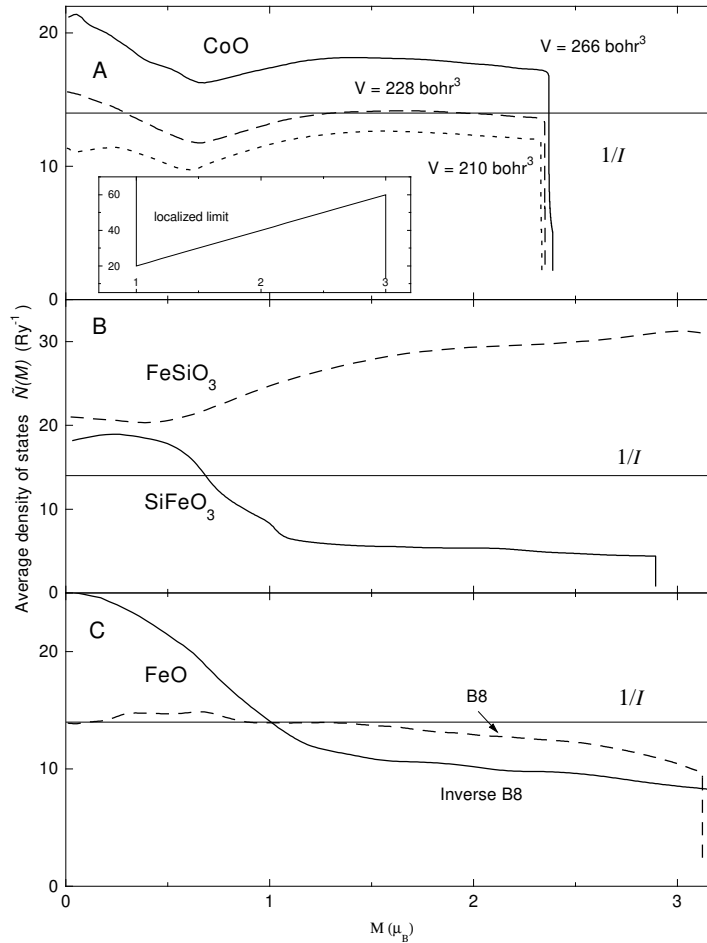


Fig. 1. – Stoner diagram for (a) CoO in the NaCl (B1) structure with a cubic lattice (b) FeSiO₃ in the cubic perovskite structure, and (c) FeO in the NiAs structure. The effective density of states is plotted against moment for several different volumes. The inverse Stoner parameter, $1/I$ is also shown, and places where the effective density of states crosses $1/I$ with a negative slope are stable solutions. At high volumes (low pressures) there is only a high-spin (large moment) solution. At intermediate pressures both high-spin and low-spin solutions exist. (Whether such coexistence is possible, i.e. whether the transition is first-order or second-order, depends on the shape of the effective density of states.) At high pressures, there is only a low-spin solution. The Stoner model behaves very differently from the localized, crystal field, picture (shown in inset) which predicts a discontinuous transition, never giving intermediate moments. From ref. [4].

LDA, or generalized gradient approximation, GGA [7]) predicts them to be metals, but they are actually insulators. Materials which are insulating because they have magnetic correlations are known as Mott insulators [8]. In contrast to density functional theory (DFT) calculations within LDA or GGA, Hartree-Fock theory gives a large band gap for transition metals oxides [9], much larger than the experimentally observed gaps. It is generally understood that the the problem with LDA and similar theories for these materials is that they underestimate the local Coulomb repulsions between electrons. Band theory assumes that electrons are delocalized through space, but if the electrons can be considered as localized, the energy will depend on how many electrons are on a given site (i.e. localized on a given atom or region of space). In order to conduct electricity the energy cost for an electron to move from site to site cannot be too high. There are several approaches that give a insulating behavior for the problematic transition metal oxides.

In the simplest one-band Hubbard model, the Hamiltonian is given by

$$(7) \quad E = T \sum_{ij} (c_{i\uparrow}^\dagger c_{j\uparrow} + c_{i\downarrow}^\dagger c_{j\downarrow}) + U \sum_i n_{i\uparrow} n_{i\downarrow}$$

and the band states are split into an upper and lower Hubbard band, with a splitting of U . The first term is the hopping, or hybridization, governed by T . The creation operator c_i adds an electron to site i , and the destruction operator c_i^\dagger subtracts an electron from site i . The number of up electrons on site i is

$$(8) \quad n_{i\uparrow} = c_{i\uparrow}^\dagger c_{i\uparrow},$$

and similarly for the down electrons. In this simple model there can be 0, 1 (up or down), or 2 (one up and one down) electrons on a site. Even this simple model has never been solved exactly in three dimensions. The physical picture, however, is clear. The first term is the band term. The second is a local repulsion. A local repulsion between electrons can open up a gap in the excitation spectrum, and make a insulator out of a band metal.

1.2.1. LDA+U. One approach that gives an insulating ground state for transition metal oxides is the LDA+U model, which adds a Hartree-Fock-like local Coulomb repulsion tensor U and exchange interaction J , and then attempts to correct for double counting. The LDA+U model has given excellent results for a variety of systems [10, 11, 12, 13], but the limits of the model are still not well known, for example whether it properly predicts the high pressure behavior of Mott insulators. Modern LDA+U is rotationally invariant, but still has some dependence of the choice of local orbitals in which to apply the corrections. The rotationally invariant LDA+U contribution to the energy is given by

$$\Delta E = \frac{1}{2} \sum_{m_1 m'_1 m_2 m'_2 \sigma} U_{m_1 m_2 m'_1 m'_2} (n_{m_1 m_2}^\sigma - \bar{n}_{m_1 m_2}) (n_{m'_1 m'_2}^{-\sigma} - \bar{n}_{m'_1 m'_2}) +$$

$$\begin{aligned}
& + \frac{1}{2} \sum_{m_1 m'_1 m_2 m'_2 \sigma} (U_{m_1 m_2 m'_1 m'_2} - J_{m_1 m_2 m'_1 m'_2}) (n_{m_1 m_2}^\sigma - \bar{n}_{m_1 m_2}) (n_{m'_1 m'_2}^\sigma - \bar{n}_{m'_1 m'_2}) - E_{DC} \\
(9)
\end{aligned}$$

where E_{DC} is the double counting correction accounting for the on-site Coulomb interaction already included in LDA. The tensors U and J are the Coulomb and exchange integrals between electrons in orbitals m_i . The n 's are the site occupancy matrices and σ designates spin. For the double counting correction, we use the form:

$$(10) \quad E_H^{Model} = \frac{1}{2} \bar{U} 2\bar{n}(2\bar{n} - 1) - \frac{1}{2} \bar{J} [\bar{n}^\uparrow (\bar{n}^\uparrow - 1) + \bar{n}^\downarrow (\bar{n}^\downarrow - 1)].$$

where

$$\begin{aligned}
\bar{U} &= \frac{1}{(2l+1)^2} \sum_{mm'} \langle mm' | \frac{1}{r} | mm' \rangle \\
\bar{J} &= \bar{U} - \frac{1}{2l(2l+1)} \sum_{mm'} (\langle mm' | \frac{1}{r} | mm' \rangle - \langle mm' | \frac{1}{r} | m' m \rangle) \\
(11)
\end{aligned}$$

and where $\bar{n}^\sigma = \sum_m n_{mm}^\sigma$, and $\bar{n} = (\bar{n}^\uparrow + \bar{n}^\downarrow)/2$. The Coulomb and exchange tensors U and J are defined by

$$\begin{aligned}
U_{m_1 m_2 m'_1 m'_2} &= \langle m_1 m'_1 | \frac{1}{r} | m_2 m'_2 \rangle \\
(12) \quad J_{m_1 m_2 m'_1 m'_2} &= \langle m_1 m'_1 | \frac{1}{r} | m'_2 m_2 \rangle,
\end{aligned}$$

and are to be evaluated over localized orbitals. In practice U and J are input parameters, but can be determined from constrained occupancy computations [13, 57]. Actually the Slater integrals F_0 , F_2 , and F_3 are input for d -states, and $U = F_0$, $J = F_2 + F_4/14$, and $F_2/F_4 = 0.625$. We use the atomic values for F_2 and F_3 : $F_2=8.18$ eV and $F_4=5.15$ eV, or $J=0.95$ eV, for CoO and $F_2=7.67$ eV and $F_4=4.79$ eV, or $J=0.89$ eV for FeO.

LDA+U has been shown to give good predictions of the electronic structure of NiO [13, 14, 16]. In ref. [14] the equation of state and elastic constants for cubic NiO were computed with LDA+U and SIC (see below), and reasonable agreement with experiment was found. However, there have been few tests of LDA+U total energies, and here we study in detail the energetics with respect to strain and compression in FeO.

1.2.2. Self-interaction corrections. Another successful model, which still has not been fully explored for Mott insulators, is known as the self-interaction correction (SIC). This is understood easiest by considering a hydrogen atom with one electron. The self-consistent field electrostatic energy and Hartree self-consistent potential are computed from the electronic charge density. The charge density for a hydrogen atom is spread

out, yet actually an electron is only at one place at a time; there should be no electron-electron interaction when there is only one electron. The Hartree potential V_H and energy are computed from the charge density, so that

$$(13) \quad V_H(r) = \int dr'^3 \frac{\rho(r')}{|r-r'|},$$

for example, which is an electron-electron interaction, which should not be present in a hydrogen atom! The LDA exchange-correlation potential also depends on the charge density, and would be non-zero in the hydrogen atom. In the exact density functional, which is unknown, the exchange-correlation potential must exactly cancel the Hartree potential, giving zero for the total electron-electron interaction. This can be enforced, by correcting the potential so that

$$(14) \quad V_{SIC} = V_{LDA} - \sum_{ik} \int dr'^3 V(\rho_{ik})$$

where

$$(15) \quad \rho_{ik} = \psi_{ik}^* \psi_{ik}.$$

The simple SIC correction above clearly depends on the localization of the basis set. It works very well in an atom, but in a crystal the Bloch functions are extended throughout space, and the correction goes to zero. However, one can perform a unitary transformation on the orbitals and find sets of localized orbitals. It has been shown that there is a variational principle, and the most localized orbitals have the lowest SIC energy. Thus SIC computations are quite computationally intensive, as there is an inner iterative loop in which the orbitals are localized. SIC does very well for excitation energies and does predict an insulating ground state for the transition metal oxides [17, 18, 19], and gives a qualitatively correct picture for the rare earth metals [20].

In the exact density functional theory, there should be no self-interaction. One can still question whether the way SIC enforces freedom from self-interaction is realistic or accurate. For example, the weighted density approximation (WDA) is constructed to give no self-interaction per orbital, yet it makes only small changes in the electronic structure in most systems studied so far [15]. In contrast, SIC makes large changes in electronic structure for all systems studied.

LDA+U and SIC make very different predictions for the electronic structure. Whereas LDA+U pushes unoccupied states up in energy, SIC pulls occupied states down in energy. This makes a difference when there are different types of bands present. For example, in the transition metal oxides, 4s states are not affected directly by U . The nature of the band gap is thus different in the two models, as will be discussed further below. In ref. [14] the EELS spectra are computed for O 2p for LDA+U and SIC, and both compare well with each other and with experiment. However, the differences in models

is minimized by considering only the O 2p states, which are only indirectly effected by the correlations.

1.2.3. Dynamical mean field theory. Dynamical mean-field theory (DMFT) is a method for treating correlated systems that becomes exact in infinite dimensions [21]. It can be applied as an extension of LDA+U that includes a frequency dependent hybridization function [22]. A multiplet ion is solved self-consistently within the mean field Anderson impurity model. It is very time-consuming with few cases studied, and it is probably not currently tractable to study a system such as FeO using DMFT as a function of strain and pressure, as we did here. In DMFT, one still uses the parameter U .

1.2.4. Hartree-Fock. In contrast to density-functional based methods, Hartree-Fock theory gives a large band gap (way too large) for transition metal oxides, and some feel that Hartree-Fock should therefore be taken as the zeroth order method for these materials [6, 23, 9]. This is indeed the basis of the LDA+U method. Hartree-Fock by itself is not a reasonable way to study the high pressure properties of Mott insulators, because it would grossly overestimate the pressure of a metal-insulator transition, since it greatly overestimates the gap. This is because the Coulomb repulsion in Hartree-Fock is completely unscreened. Furthermore, Hartree-Fock does not work well for any metal, always predicting a singularity in the density of states at the Fermi level. Thus it is not a good way to study metal/insulator transitions.

2. – Methods

We have used a variety of methods to study Fe, FeO and CoO, and only a brief outline of the methods will be given here. Computational details are given in the referenced papers. For Fe our most accurate method is the Linearized Augmented Plane Wave (LAPW) method. We have used the LAPW method to study non-magnetic and collinear magnetic properties of Fe [24, 25, 26]. LAPW is a full-potential all-electron (i.e. no pseudopotential) method, and the basis is very flexible, and is suited both to the interstitial region and the atomic cores. One advantage of LAPW is that it is straightforward to converge the results with respect to basis set size. Our computations are done using the Generalized Gradient Approximation (GGA) for the exchange-correlation potential [7].

3. – Results and Discussion

3.1. Overview of effects of pressure on magnetism. – A straightforward effect of pressure on magnetism is through structural phase transitions. Compression can drive structural phase transitions, and the magnetic properties of the different phases will be different. For example, body-centered cubic iron is ferromagnetic, and hexagonal close packed iron was believed to be non-magnetic, so the bcc to hcp transition would also be a ferromagnetic to non-magnetic transition. One can also have transitions from one magnetic

structure to another. The simplest is the Curie point, where the magnetic moments become disordered. Generally, there are still local moments on the atoms, but they are no longer ordered. The Curie temperature in bcc iron is 1043 K. One could also have a transition from ferromagnetic to antiferromagnetic, or from an ordered structure to an incommensurate structure.

As pressure is increased magnetic moments tend to decrease, and eventually magnetism is squeezed out. This can be understood in the Stoner model as due to the general increase in bandwidths with pressure, decreasing the effective density of states, whereas the effective Stoner parameter is approximately constant. This also happens in the Hubbard picture, since U is approximately constant or decreasing with pressure, and the hopping parameter T increases in magnitude with pressure. Actually the parameters of the two models are closely related. Actual computations are shown for FeO using the LAPW method and the GGA in fig. 2. Note that the magnetic behavior with pressure depends strongly on the crystal structure (cubic lattice versus one with a small rhombohedral strain) and on the magnetic order (antiferromagnetic versus ferromagnetic). The antiferromagnetic state with cubic lattice shows a strong first-order high-spin low-spin transition with an appreciable ΔV of 8%. With a rhombohedral strain, or with ferromagnetic order, the transition is gradual. This kind of comparison is one of the useful things that can be done with theory. In experiments one is generally stuck with the lowest free energy phase unless there is a large activation energy so that metastable phases can be studied. With theory one can answer the question, “What if FeO was ferromagnetic?” High-spin low-spin transitions are predicted in all the transition metal oxides [4, 27], and have been observed in sulfides and f-metals [28].

Metals such as Co and hcp Fe do not show discontinuous transitions in our computations, but show a gradual reduction in moments as the bands widen with increasing pressure (fig. 3)[26]. The effect of pressure on magnetism is a strong function of the magnetic structure, as well as chemical composition.

3.2. *Magnetic behavior of Fe, FeO, and CoO with increasing pressure.* –

3.2.1. Fe. There are three well-known crystalline phases for Fe, body-centered cubic (bcc, or α -Fe), which is the stable form at ambient conditions, face-centered cubic (fcc, or γ -Fe) which is stable at high temperatures, and hexagonal close-packed (hcp, or ϵ -Fe), stable at high pressures (fig. 4). There is also a small bcc field (δ -Fe) just before melting at low pressures. Bcc iron is ferromagnetic, fcc has magnetic correlations, but not an ordered magnetic structure, and hcp was believed to be non-magnetic (though see discussion below). See ref. [29] for a review of experimental studies of Fe at high pressures.

One of the well-known failures of the local density approximation (LDA) is that it gives the wrong ground state for Fe. LDA only gives the magnetic bcc phase at negative pressures, but at zero pressure gives a close-packed non-magnetic ground state. One of the early successes of the GGA was the correct prediction of the bcc ground state and an accurate transition pressure to hcp from bcc of 11 GPa [24, 30] compared with a

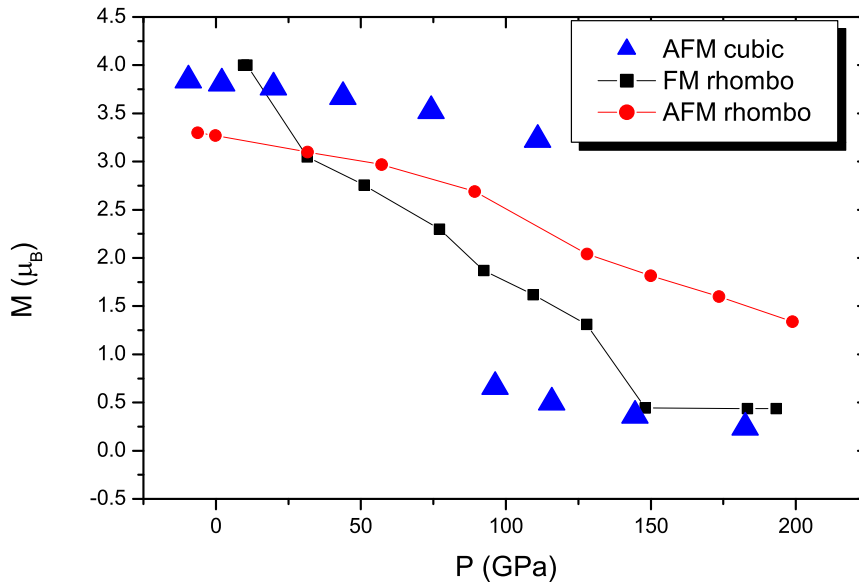


Fig. 2. – Computed magnetic moments for FeO using the LAPW method and the GGA. For the cubic lattice the antiferromagnetic solution gives a discontinuous high-spin low-spin transition. However, with the equilibrium rhombohedral distortion at each volume, the moments decrease continuously. The behavior also depends on the nature of magnetic ordering, i.e. antiferromagnetic or ferromagnetic.

10-15 GPa hysteresis loop from experiment. This showed that the GGA was accurate for the magnetic stabilization energy of bcc-Fe. Furthermore, bcc iron is only stable due to its magnetism. Non-magnetic bcc iron would not be a stable phase, except possibly in the δ -Fe field just before melting. There had been speculations that the Earth's solid inner core was bcc-iron, but calculations showed that bcc-Fe was mechanically unstable at those conditions because it was non-magnetic at such high pressures [25].

Not only is magnetism important in bcc iron, but it is also important in fcc. We tried to find the phase transition from hcp to non-magnetic fcc using the particle-in-a-cell model (ref. [31] and unpublished), but did not find a stable field for fcc below melting, which could be explained by magnetic stabilization of fcc. Experimentally, it is known that fcc iron is magnetic (i.e. has local moments).

The computed equations of state for magnetic bcc-Fe, and non-magnetic fcc and hcp, are shown in fig. 5. The inset shows the total energies for these three phases; the transition from bcc to hcp occurs at the common tangent. The computed P-V equation of state is in good agreement at high pressures, and with bcc, but discrepancies are seen at lower pressures; the non-magnetic hcp equation of state is too stiff at low pressures.

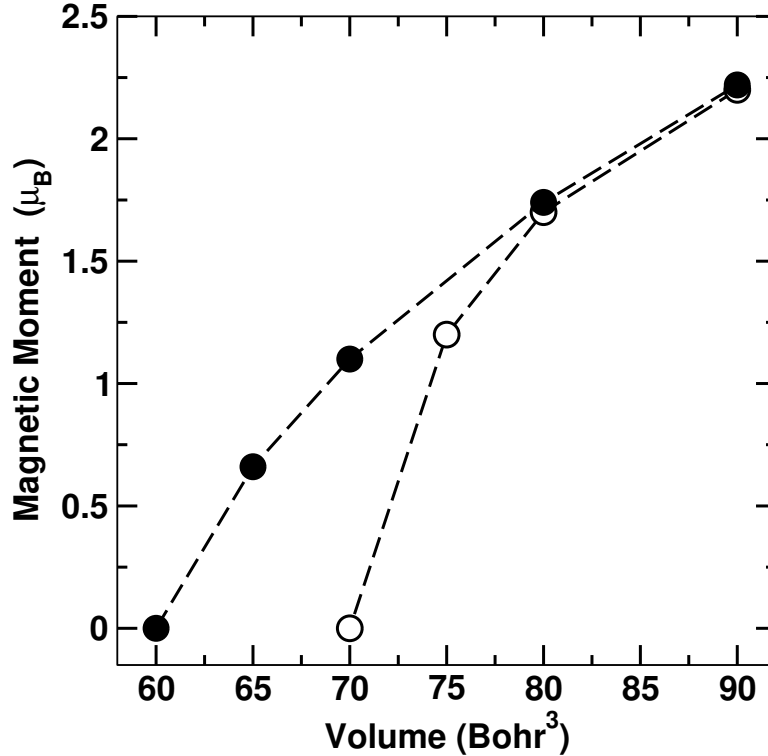


Fig. 3. – Computed magnetic moments for afmI (open symbols) and afmII hcp Fe. These are the moments in the muffin tins, which have a radius of 2.0 bohr. Note that in the original presentation of these results (ref. [26]) the moments were plotted incorrectly smaller by a factor of two.

The discrepancy at low pressures seems very large if one compares the zero pressure bulk modulus K_0 from the equation of state. The experimental value is 165 GPa, compared with 292 GPa from the GGA equation of state. K_0 is a fictive quantity for hcp-Fe, since it has not proved possible to quench hcp-Fe to zero pressure, but nevertheless the discrepancy seems larger than expected compared with GGA results for other hcp transition metals (for example for Co $K_0=190$ GPa from experiment and 212 GPa from GGA, and Re is 365 GPa from experiment and 344 GPa from GGA [26]).

Disagreements between theory and experiment often lead to advancement in theory, or in our understanding of physics. In this case, it appears that the discrepancy in the equation of state of hcp-Fe is not due to inaccuracy of the theoretical calculations or methods, but is due to the neglect of magnetism in hcp-Fe. Experimental data had been interpreted to show no magnetism in hcp-Fe, and indeed calculations showed that ferromagnetism was not stable in hcp-Fe. Mössbauer experiments showed no evidence for ordered magnetism in hcp-Fe, even down to 0.03 K [34, 35]. However, even in the

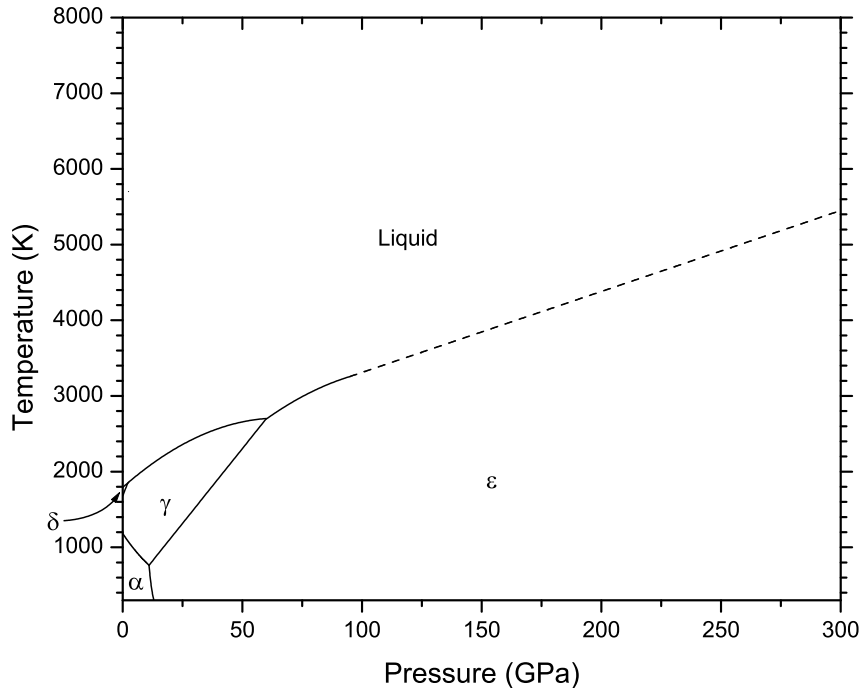


Fig. 4. – The experimental phase diagram for Fe. See ref. [29] for discussion.

earliest papers on Mössbauer in hcp-Fe it was recognized that magnetism was not ruled out by the data [36, 37]. Given the large unexplained discrepancy in the equation of state, we started looking for stable magnetic structures. Two stable antiferromagnetic hcp structures were found, and the most stable, afmII, is stable up to about 50 GPa. The computed local magnetic moments are shown in fig. 3. The afmI structure consists of layers of Fe with alternating spin along the c -axis. The afmII structure (fig. 6) alternates spin-up and spin-down layers along the hexagonal a -axis [26].

The bulk modulus K_0 for afmII hcp-Fe is 209 GPa, a vast improvement from the non-magnetic GGA value of 292 GPa, but higher than the experimental value of 165 GPa. Another piece of evidence for local antiferromagnetic correlations comes from Raman spectroscopy. The hcp structure has a single Raman active mode. Raman experiments on hcp-Fe show a second broad peak [38] which cannot be explained within hcp symmetry. The afmII structure has magnetic symmetry lower than hcp, is orthorhombic, and has two transverse optic Raman modes. It is very interesting that the predicted splitting in Raman frequencies due to the antiferromagnetic order for afmII [38] is in excellent agreement with experiment (fig. 7). However, the second peak seen in experiments is

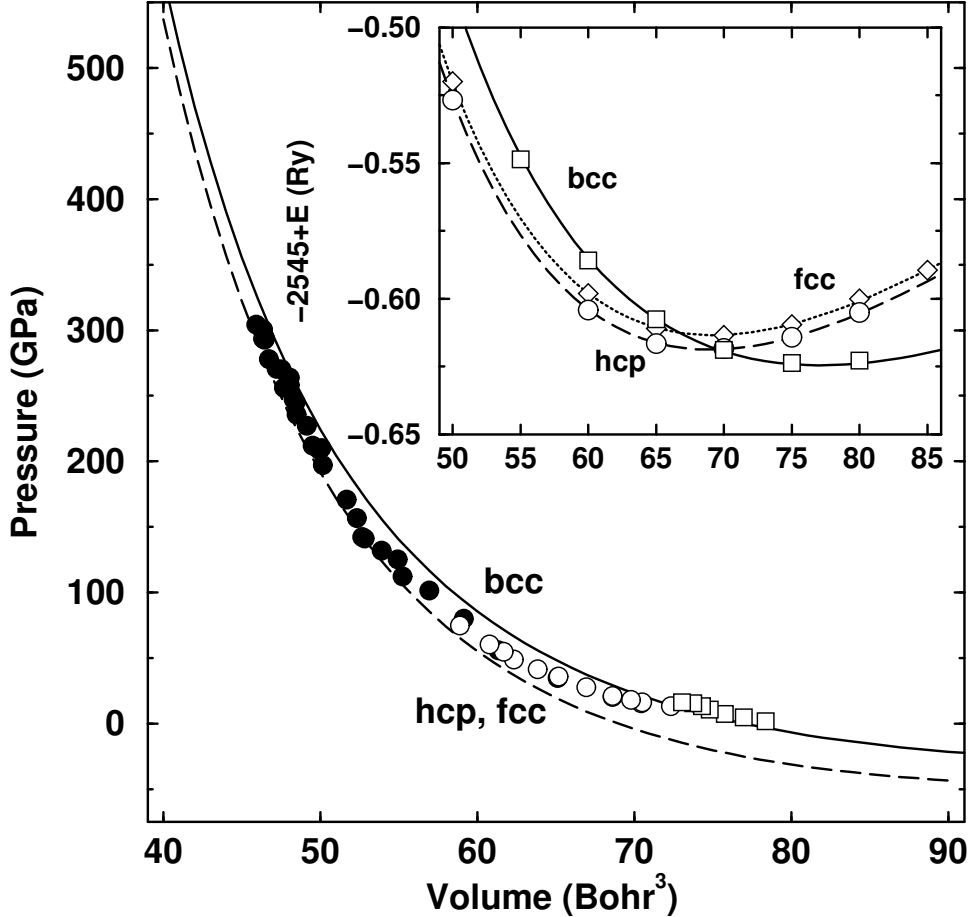


Fig. 5. – Computed equation of state for Fe using the LAPW method and GGA. A transition pressure from bcc to hcp of 11 GPa is obtained from the common tangent of the energy curves shown in the inset, in good agreement with experiment. The computed PV equation of state is in good agreement with experiments [32, 33] at high pressures, and with bcc.

quite broad, suggesting that a long-range ordered magnetic structure is not present.

The calculations we discuss next show a lower energy state which has non-collinear magnetism, but still has local antiferromagnetic order. This evidence, including the Mössbauer data, which does not show a well-ordered magnetic structure, suggests that there are local correlations which are limited in spatial extent, and/or are dynamic. At low temperatures a spin glass may form. Since fcc iron has a non-collinear structure[39], and since Mössbauer data does not show an ordered structure, we decided to look for non-collinear magnetism in hcp iron. This can be done self-consistently [40], but since we were also interested in simulating high temperature properties, we used a faster method consisting of an accurate tight-binding model fit to first-principles GGA calculations

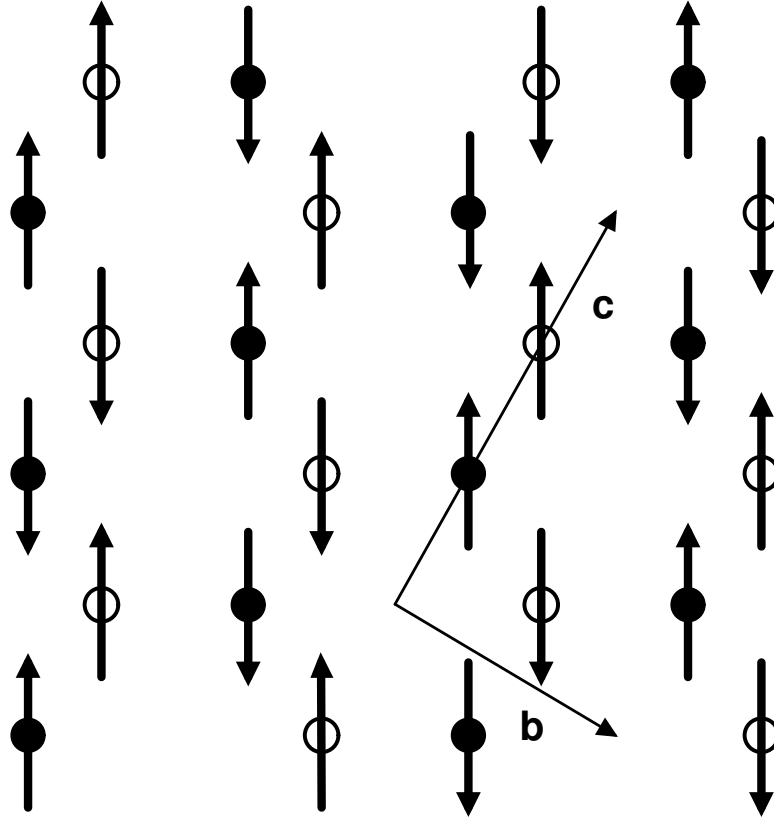


Fig. 6. – Antiferromagnetic groundstate of hcp iron (afmII). Filled symbols show the atomic positions at $z=1/4$, the open symbols at $z=3/4$ with the arrows indicating the direction of spin on the atoms. The spacegroup of the afmII structure is $Pmma$ with the atomic positions of the spin up states at $(1/4,0,1/3)$ and spin down states at $(1/4,1/2,5/6)$. Also shown are the orthorhombic unit cell vectors in the x-y-plane (b and c): we chose the orthorhombic a -axis along the hexagonal c -axis (out of the plane). The orthorhombic b axis then coincides with hexagonal a . The orthorhombic b and c also define the eigenvectors for the displacements of the zone center TO modes (TO_b and TO_c) in the afmII structure.

[3, 31], and a non-collinear tight-binding model for the magnetism, described above. The parameter I is obtained by fitting the magnetization energies to LAPW results. The magnetization energy and moments are shown for bcc-Fe in fig. 8. Even without varying I , close agreement is obtained with the self-consistent LAPW results, except in the high pressure region where the moment drops more rapidly with increasing pressure in the model than in the self-consistent calculations. Increasing I with pressure gives good agreement with the moments and total energies.

The fcc phase is more complicated, because the q-vector of the magnetic instability varies with volume. Tight-binding model calculations reproduce this behavior (fig. 9).

For hcp Fe, we did find a non-collinear magnetic structure more stable than the

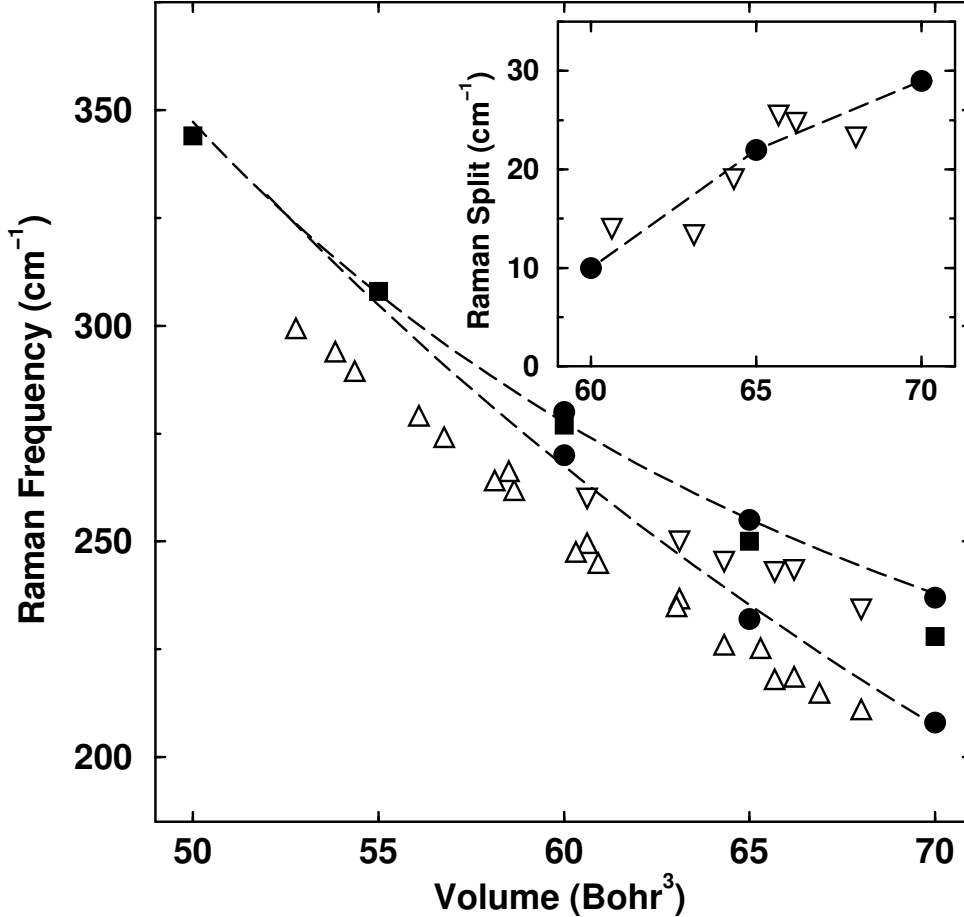


Fig. 7. – Transverse optical frequencies as a function of atomic volume. Non-magnetic calculations are shown in filled squares. The afmII structure has two transverse optical modes (filled circles) with TO_b being the lower and TO_c the upper branch. The dashed lines through TO_b and TO_c are finite strain fits to the results to third order in $V^{-2/3}$. Experiments [38] identify two peaks in the Raman spectra up to 40 GPa. The stronger, low frequency peak is shown with triangles up, the weaker, high frequency peak with triangles down. The inset compares the calculated split in TO frequencies (circles) with the Raman experiment (triangles).

collinear afmII structure (Table I). The afm structures are frustrated; it is impossible to get a perfectly ordered antiferromagnetic hcp structure. The non-collinear structure reaches a compromise, with spins either antiparallel, or perpendicular (fig. 10). The equation of state is vastly improved using the non-collinear magnetization, and is in as good agreement with experiment as is typical for first-principles methods II.

There is increasing theoretical evidence that hcp-Fe has local magnetic moments, which are not long-range ordered, but have strong local antiferromagnetic, non-collinear,

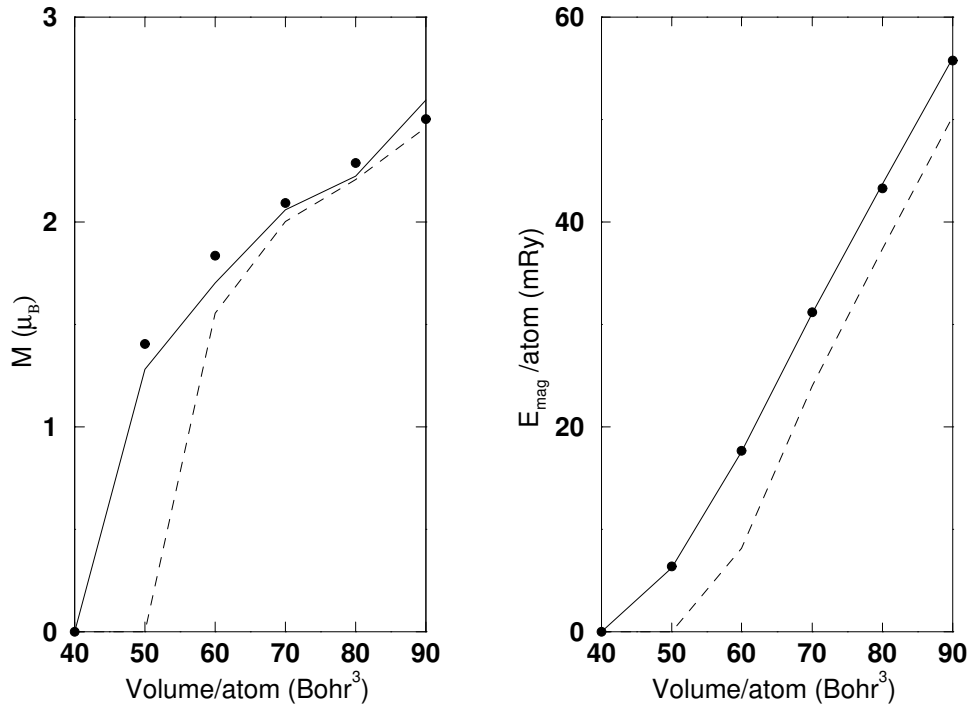


Fig. 8. – Magnetic moment and magnetization energy for bcc iron. The points are computed using LAPW [24]. The dashed line is using a single value of $I = 0.95$ eV. The solid line is obtained letting I vary as a function of volume, and fitting to the LAPW magnetization energies.

correlations. On the other hand, experiments suggest that hcp-Fe is non-magnetic. Mössbauer data show no ordered moments, requiring a correlation time less than 10^{-7} - 10^{-9} seconds. X-ray absorption experiments [43] also show significant decrease of moment between bcc and hcp, but they do not prove complete loss of magnetism; the change in the absorption spectrum is due to changes in density of states as well as changes in the spin-related satellite. Recent experiments that show superconductivity in hcp-Fe [44] are fascinating. (However, the data reported in ref. [44] do not prove superconductivity unambiguously; they could alternatively be interpreted as a magnetic phase transition. But they are strong evidence for superconductivity given the strong dependence of the resistivity of applied magnetic field.) It used to be thought that superconductivity and magnetism were incompatible, but that is now known to be not always true, and weak magnetism may promote exotic superconductivity [45]. Nevertheless, the fact that only specially treated samples were superconducting suggests that the superconductivity in Fe may be exotic. The main problem with the idea that hcp Fe is locally magnetic are the Mössbauer measurements. It is hard to understand how at the lowest temperatures the spin dynamics would still be so rapid as to show no magnetism. On the other hand, it is rare for band theory to incorrectly predict a magnetic ground state. Including local

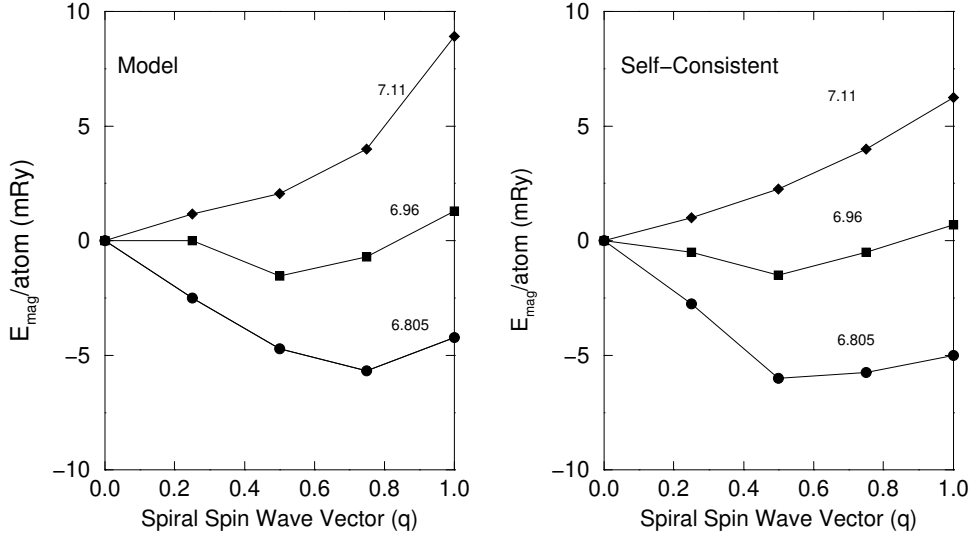


Fig. 9. – Energy versus spiral spin vector for fcc iron. The tight-binding model results are in good agreement with those obtained self-consistently [42].

correlations neglected in GGA should further promote magnetism. If there were structural distortions or very soft vibrational modes that invalidate the Born-Oppenheimer approximation there would be some grounds for considering the theoretical predictions less firm. But hcp is a very simple, close-packed structure, so that an incorrect prediction of a magnetic ground state does not seem reasonable. Furthermore, as shown above, including magnetism greatly improves the equation of state of Fe. So there remains a problem reconciling the experimental and theoretical evidence.

One possible explanation comes from our exploration of non-collinear magnetic struc-

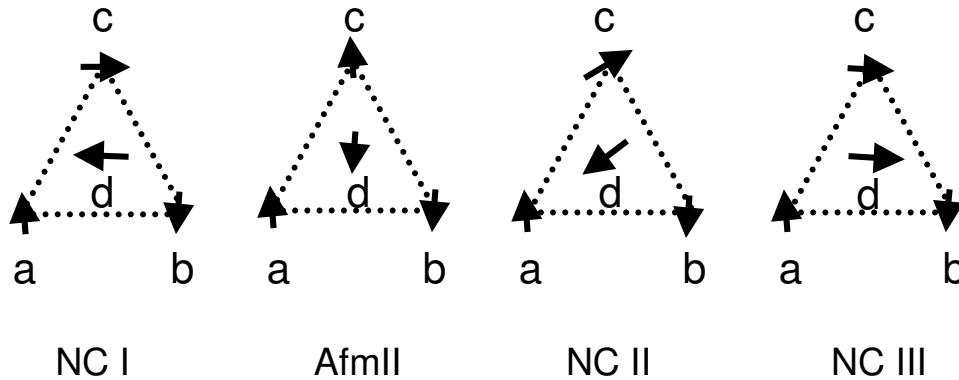


Fig. 10. – Comparison of ground state non-collinear structure and afmII structure.

TABLE I. – *Magnetization energy(mRy) for different atomic volumes V (Bohr³). The value of Stoner parameter I (eV) for the different volumes is given in the first column. The c/a ratio for the atomic volumes lie between 1.585 and 1.59. The magnetic moments for the ground state are given in parenthesis.*

I	V	Ferro	NC I	afmII	NC II	NC III
1.01	90	26.8	20.9(2.4)	19.4	20.6	21.6
1.05	80	2.1	11.2(2.1)	8.9	10.9	11.1
1.1	75	0	9.2(1.9)	6.2	7.9	6.5
1.14	70	0	5.80(1.7)	3.1	4.5	2.9
1.19	65	0	2.9(1.4)	0.5	2.7	0

tures in hcp. We find that most disordered arrangements of moments give a self-consistent solution with no moment. Certain ordered structures give stable moments. Perhaps defects or thermal excitations can disorder the moments enough to force the moments to zero. Perhaps the ordered ground states we predict will only be seen in very pure samples, similar to the purity requirement needed for superconductivity.

3.2.2. FeO and CoO. Transition metal oxides like FeO and CoO present an even more challenging problem to both theory and experiment. Understanding materials such as FeO is one of the frontier problems in condensed matter physics. FeO and CoO are Mott insulators, that is they are insulating because of local magnetic moments. Conventional band theory makes FeO and CoO metals [46], and no small change in exchange-correlation potential will make them insulators. (Large changes in the exchange correlation potential can make them insulators, but at the expense of accurate total energies [47].) In spite of this failure, conventional LDA or GGA calculations predict energetic properties, such as equations of state, and the magnetic moments reasonably well [48]. LDA+U predicts a band gap and the canted magnetic moments and lattice strains experimentally observed in CoO are reproduced [49].

We have performed LDA+U computations on CoO and FeO and get very encouraging results, but only with more experiments will the predictive power of LDA+U be understood. Since the results depend on the value of U , how U is computed or estimated is critical. Without comparison with experiment it is hard to test different models for U , so we have used several different values. A complication of LDA+U is that different

TABLE II. – *Comparison of experimental and theoretical values of equilibrium volume (V_0) and bulk modulus (K_0) for ϵ -Fe.*

Fe(GGA)	V_0 (Bohr ³)	K_0 (GPa)
Expt[33, 32]	75.4	165
Non-Magnetic[26]	69.0	292
Collinear (afmII)[26]	71.2	209
Non-Collinear	72.3	177

self-consistent results can be obtained depending on electronic symmetry and d-state occupations. Thus one can have electronic symmetry that is lower than the lattice or magnetic symmetry due to the orbital ordering. We report results on the lowest energy states we have found, but no systematic study of the different metastable states has yet been made.

The equations of state for CoO obtained using LDA+U (and the GGA, i.e. $U = 0$) are reasonable (fig. 11), and a U from 2-5 eV is consistent with the experimental equation of state. Figure 12 shows the computed magnetic moments for antiferromagnetic CoO with a cubic lattice, computed using LMTO-ASA with GGA. The curve for $U = 0$ is the GGA result. Note that our LDA+U results used GGA for the density functional, so our results could properly be called GGA+U. GGA gives a high-spin low-spin transition, as we found earlier [4].

The band gap in CoO is predicted to initially increase with pressure, and then decrease. At zero pressure, the lowest conduction states are 4s states, so that the gap is an intra-atomic gap between 3d and 4s. As pressure increases, the 4s states are driven up and the gap becomes a d-d gap, which then decreases with increasing pressure. LDA+U pushes unoccupied states up into the conduction band, so that the conduction band edge contains 4s character, which are not affected by U . The d-s nature of the gap was pointed out in ref. [50]; they suggested that this is consistent with photoemission data. In contrast, SIC lowers the occupied states, rather than raising the unoccupied states, and gives a prediction of d-character for the lowest conduction band states [18]. This suggests that LDA+U may be a better approximation for the nature of the gap in transition metal oxides than SIC.

Of critical importance for gap closure, that is metallization pressure, is the behavior of U with pressure. The assumption is generally made that U is about constant with pressure, being a local, atomic-like property, but it may decrease with strong compression. In that light, the $U=2$ eV result of 170 GPa would be a lower bound for the metallization pressure for cubic CoO. Lattice distortion may increase this to higher pressure, as would a higher value of U . It is interesting that such moderate values of U are sufficient to give an insulating state over a wide range of compression, when the GGA itself gives a metallic band structure.

At high pressures and temperatures, FeO transforms from the rhombohedrally distorted rocksalt (B1) structure to a superlattice of NiAs and anti-NiAs structure [52, 53, 54]. However, at room temperature, FeO can be maintained in the distorted B1 structure to over 120 GPa [56]. Here we discuss the behavior of FeO in the distorted rocksalt structure, since understanding the behavior of transition metal oxides in this simple structure is a prerequisite to understanding the behavior of more complex phases. We have performed a large number of self-consistent computations using the full potential LMTO method [22] for different lattice strains and d-orbital occupancies. The lowest energy state we find has rhombohedral symmetry, except for very high pressures with $U = 4.6$ eV (fig. 14). This value of U was obtained by computing the change in eigenvalues with potential shift in each d-orbital, and is probably the best estimate at zero pressure [57]. As mentioned above, the effects of pressure on U are still unknown. Smaller values of U

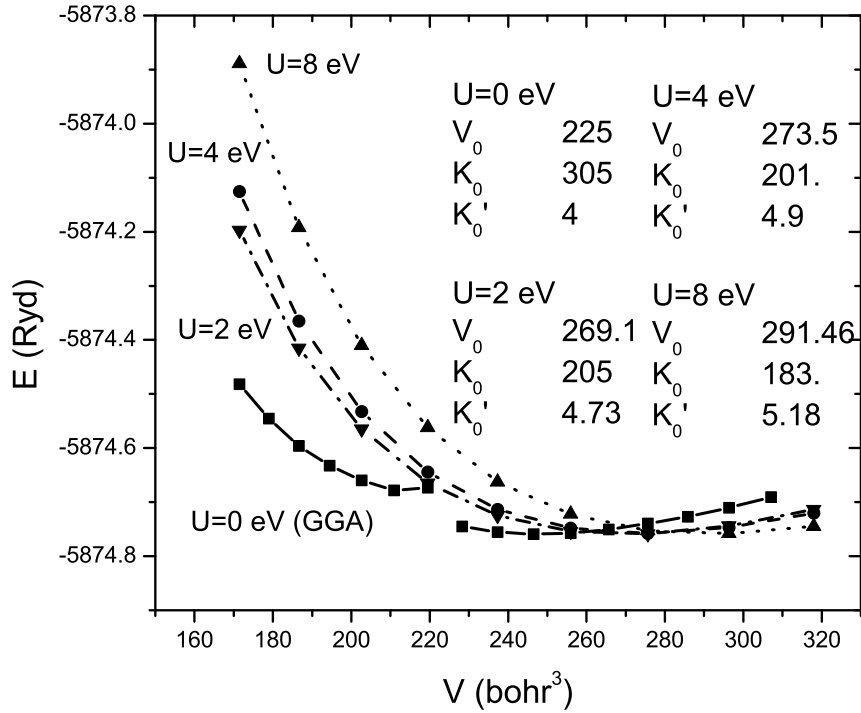


Fig. 11. – Computed equation of state for CoO and equation of state parameters from a Vinet equation [51] fit to the computed energies. The experimental values for the zero pressure volume and bulk modulus are 261 bohr³ and 181 GPa, respectively.

($U \leq 3.5$ eV) give a metallic band structure at zero pressure.

The GGA ($U = 0$) density of states is shown in fig. 15 at the experimental zero pressure volume. The electronic structure is metallic in the GGA. With a rhombohedral strain, some minority spin states move down, making it possible to open a gap, but still a gap does not form. LDA+U does open a gap (fig. 16), as was shown in the original LDA+U work (ref. [10]). LDA+U also does a much better job for an isolated Fe ion in MgO, indicating that it might work for arbitrary transition metal ion concentrations [55].

Previous work has not examined the LDA+U total energies. In order to understand how predictive are the total energies computed with LDA+U, we studied the energy as a function of rhombohedral strain for FeO. The lattice strain A in terms of the rhombo-

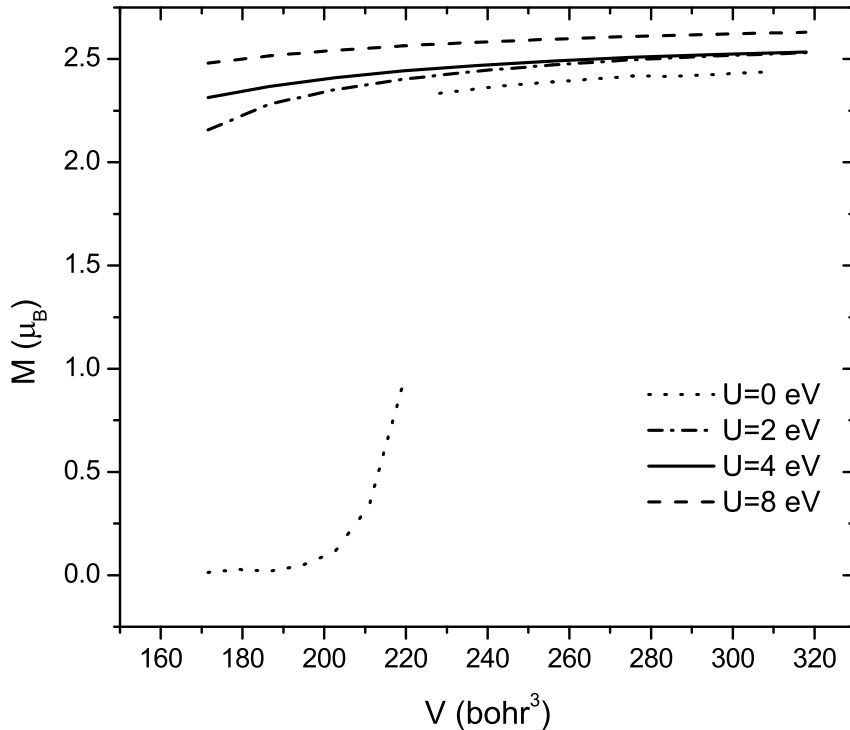


Fig. 12. – Computed local moments for Co in cubic CoO. $U=0$ is the GGA result, which shows a first-order high-spin low-spin transition. Note that turning on U inhibits the transition.

hedral strain parameter δ is given by

$$(16) \quad A = (1 + 3\delta)^{-\frac{1}{3}} \begin{bmatrix} 1 + \delta & \delta & \delta \\ \delta & 1 + \delta & \delta \\ \delta & \delta & 1 + \delta \end{bmatrix}$$

We find that the lattice strain and its pressure dependence are predicted better by LDA+ U than by GGA or LDA (fig. 17). This is strong evidence that LDA+ U is making the right kind of corrections since the energetics of strain are quite subtle.

We also found more than one stable state for FeO with different orbital occupancies. The lowest energy state at low pressures was the strained lattice with rhombohedral symmetry. At high pressures, when $U \geq 4.6$ eV, we find a phase transition to a state with monoclinic electronic symmetry (fig. 14).

The band gaps for different symmetry solutions are shown in fig. 18. The lower

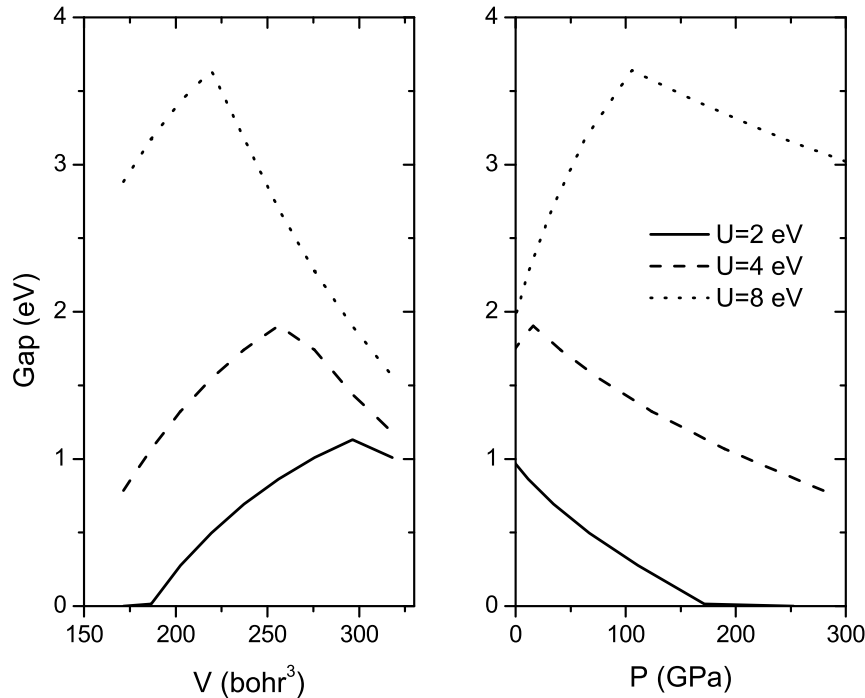


Fig. 13. – Computed band gap for cubic CoO using LDA+U.

energy rhombohedral symmetry d-state occupancies also have a larger band gap, and gap closure occurs at about 250 GPa for $U=4.6$ eV. The rhombohedral strain lowers the gap appreciably. It is interesting to note that the monoclinic structure gap closes at much lower pressures. This suggests that large non-hydrostatic stresses might promote gap closure at lower pressures than under hydrostatic conditions.

4. – Conclusions

Magnetism is an important contribution to the high pressure properties of many materials containing transition metals. For pure Fe, conventional electronic structure methods within the density functional theory using modern exchange-correlation functionals, such as the generalized gradient approximation (GGA), successfully predict structural and magnetic properties, including equations of state, phase transition pressures, elasticity, etc. There are still some areas with discrepancies, such as the elastic properties of hcp Fe, but these differences are probably due both to experimental difficulties, and to not yet having the proper magnetic structure in the first-principles computations. Discrepancies

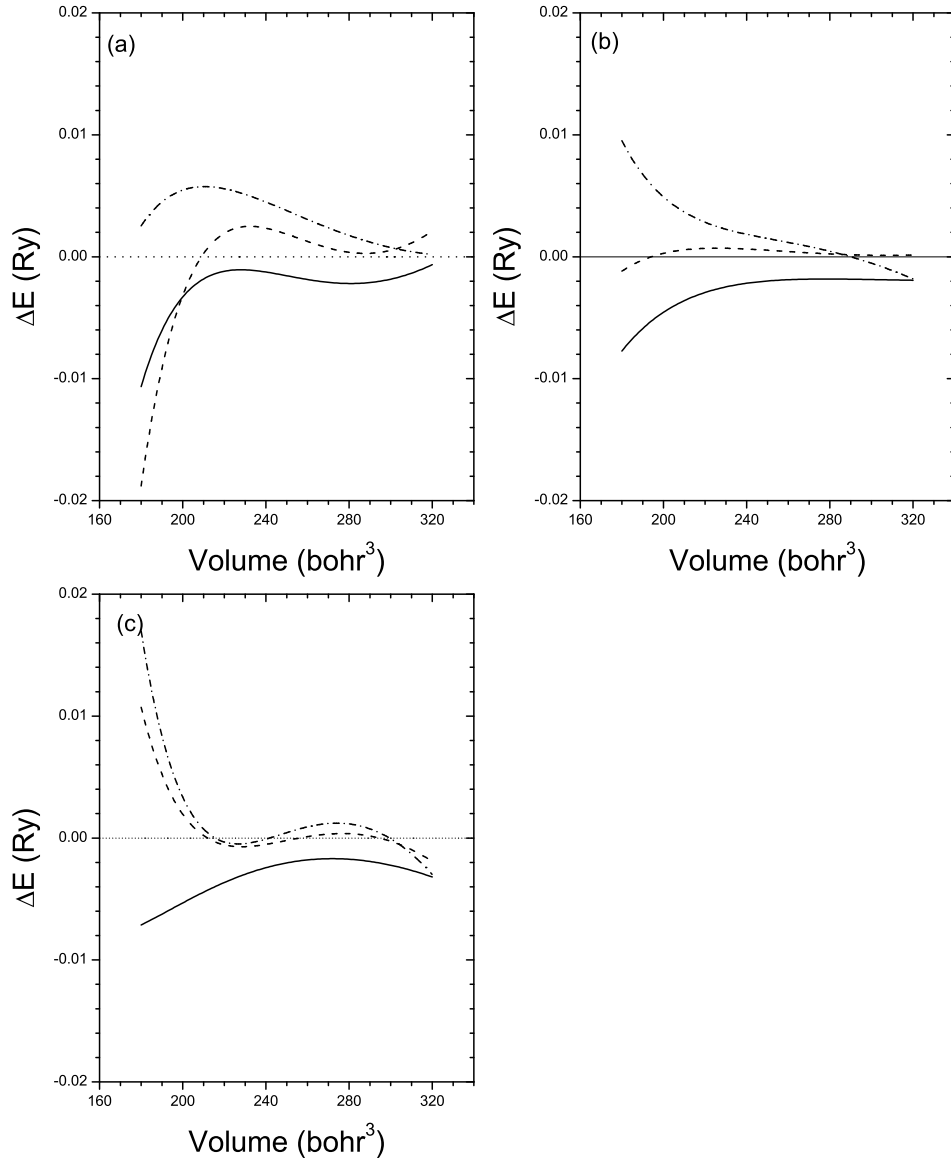


Fig. 14. – Energy differences between various LDA + U solutions and the unstrained rhombohedral solution (dotted line) for (a) $U = 4.6$ eV, (b) $U = 6.0$ eV, and (c) $U = 8.0$ eV. Solid line, strained rhombohedral solution; dashed line, strained monoclinic solution; dash-dot line, unstrained monoclinic solution.

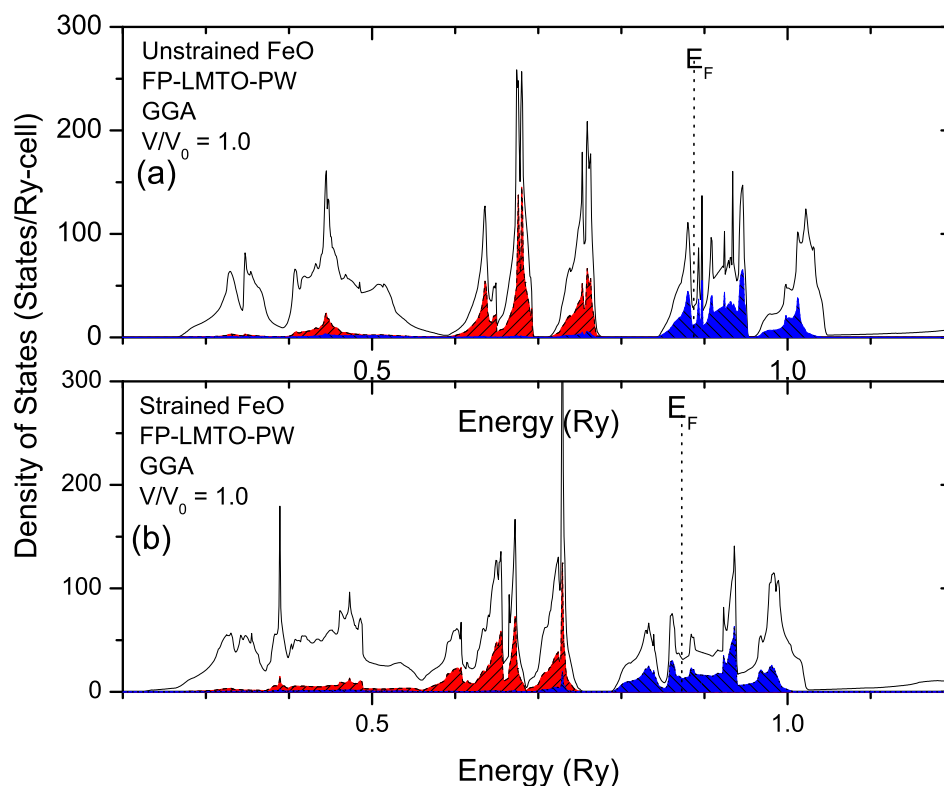


Fig. 15. – Densities of states for FeO at the zero pressure volume for (a) cubic lattice and (b) optimal rhombohedral strain computed using GGA ($U = 0$). Right-hashing, spin-up states in one Fe muffin tin; left hashing, spin-down states.

in theoretical computations of the melting curve [58, 59] are probably due to the difficulties of sufficient accuracy in computing the solid and liquid free energies rather than any fundamental problem with the underlying theory. The main remaining hurdle for Fe is to be able to do computations with sufficient speed and accuracy, self-consistently within the GGA, to compute free energies of all of the phases as functions of V , T , strain, etc., in order to obtain a thermal equation of state, elasticity, phase transitions, magnetic, and vibrational properties over a wide pressure and temperature range, though much progress has been made [58, 59, 60, 61, 62]. Theory suggests that non-collinear magnetism in Fe is key to understanding the high pressure behavior of Fe, for pressures at least up to 50 GPa. On the other hand, there are no experiments that show ambiguously the presence of local moments in hcp Fe, and many experiments imply the opposite. If indeed iron

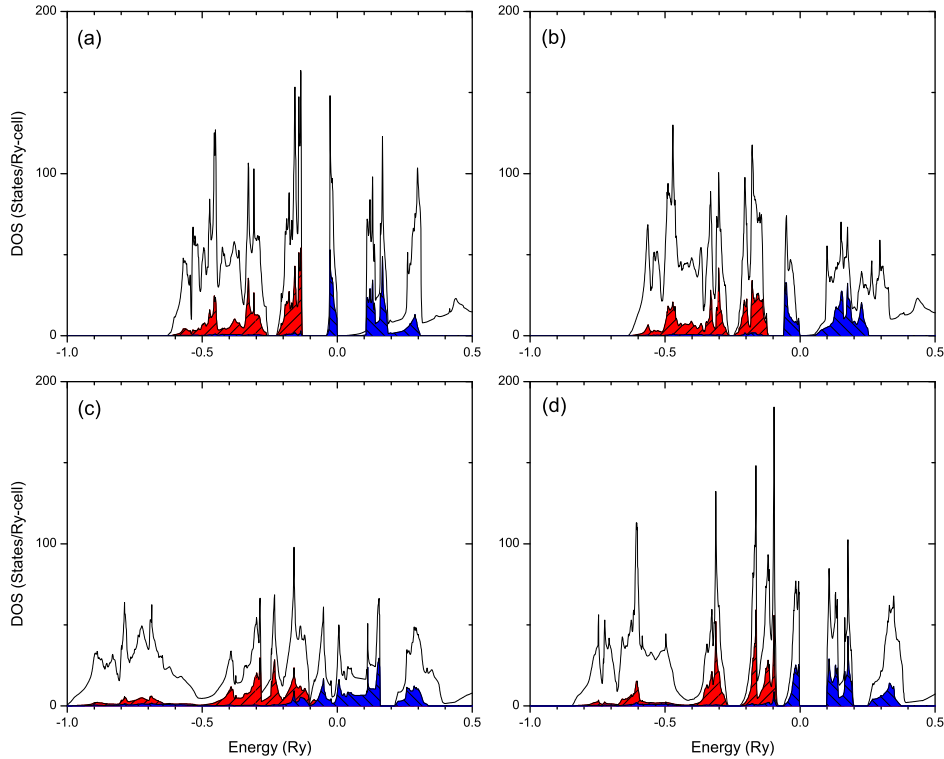


Fig. 16. – Density of states for FeO with LDA+U, and $U=4.6$ eV. (a) Rhombohedrally strained with rhombohedral electronic symmetry at 0 GPa; (b) rhombohedrally strained with electronic monoclinic symmetry at 0 GPa; (c) rhombohedrally strained with rhombohedral electronic symmetry at 180 GPa; (d) rhombohedral symmetry with a cubic lattice at 180 GPa. Right-hashing, spin-up states in one Fe muffin tin; left hashing, spin-down states.

is non-magnetic, contrary to our best theoretical calculations, important changes to our best exchange-correlation functionals are required. Alternatively, perhaps defects and/or thermal disorder is giving rise to loss of moments, as discussed above.

The situation for transition metal oxides is not so clear. Models are available now that properly give insulating behavior for FeO and other transition metal oxides, such as LDA+U and SIC. It is not yet known how predictive these methods are since the experimental data are not yet available, though computations agree well with present data. Theoretical predictions of high pressure behavior within SIC, or within other methods such as dynamical mean field theory are also not available. Here we presented predictions of behavior from LDA+U that can be tested when more experimental data

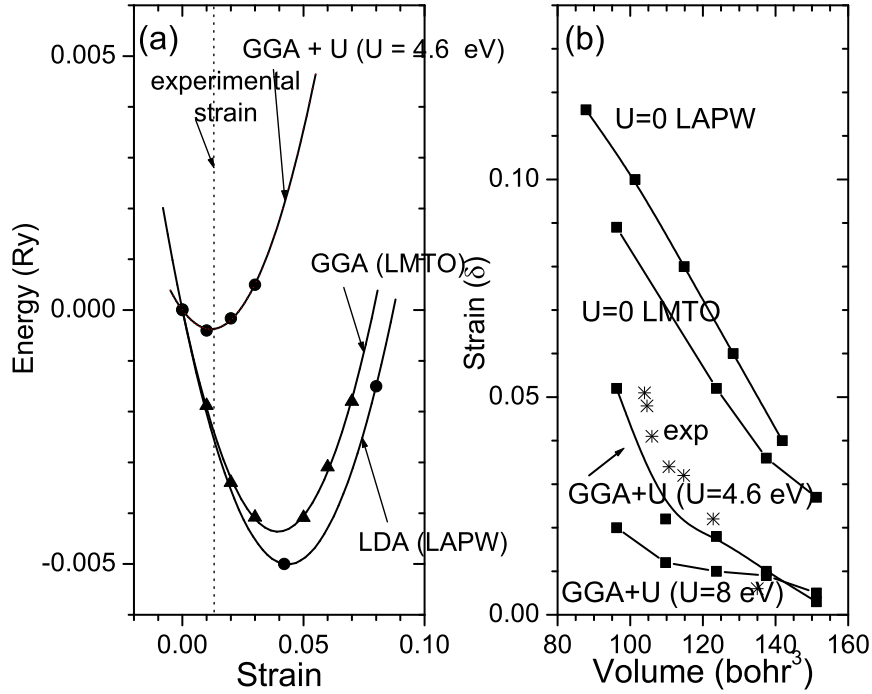


Fig. 17. – (a) Energy versus rhombohedral strain δ for FeO at $V=137.33 \text{ bohr}^3/\text{formula unit}$, the experimental zero pressure volume. The LDA+U results are an improvement over GGA. Good agreement is found between full potential LAPW and full potential LMTO, and little difference is found between LDA and GGA at fixed volume. (b) Optimized strain for FeO as a function of volume. Asterisks, experiment [56].

become available. In any case, it is clear that local magnetism is responsible for the insulating behavior, and is also probably key for accurately understanding lattice strains and elasticity.

This is a forefront area, and we expect to see many advances in both theory and experiment for the effects of magnetism on high pressure properties.

* * *

We thank B. Fultz, A. Goncharov, R.J. Hemley, A.I. Liechtenstein, H.K. Mao, I. Mazin, S. Savrasov, and V. Struzhkin for helpful discussions. This work was supported by the National Science Foundation under grants grant EAR-9870328 (REC), EAR-9614790 and EAR-9980553 (LS), and by DOE ASCI/ASAP subcontract B341492 to Caltech DOE W-7405-ENG-48 (REC). Computations were performed on the Cray SV1 at the Geophysical Laboratory, support by NSF grant EAR-9975753 and by the W. M.

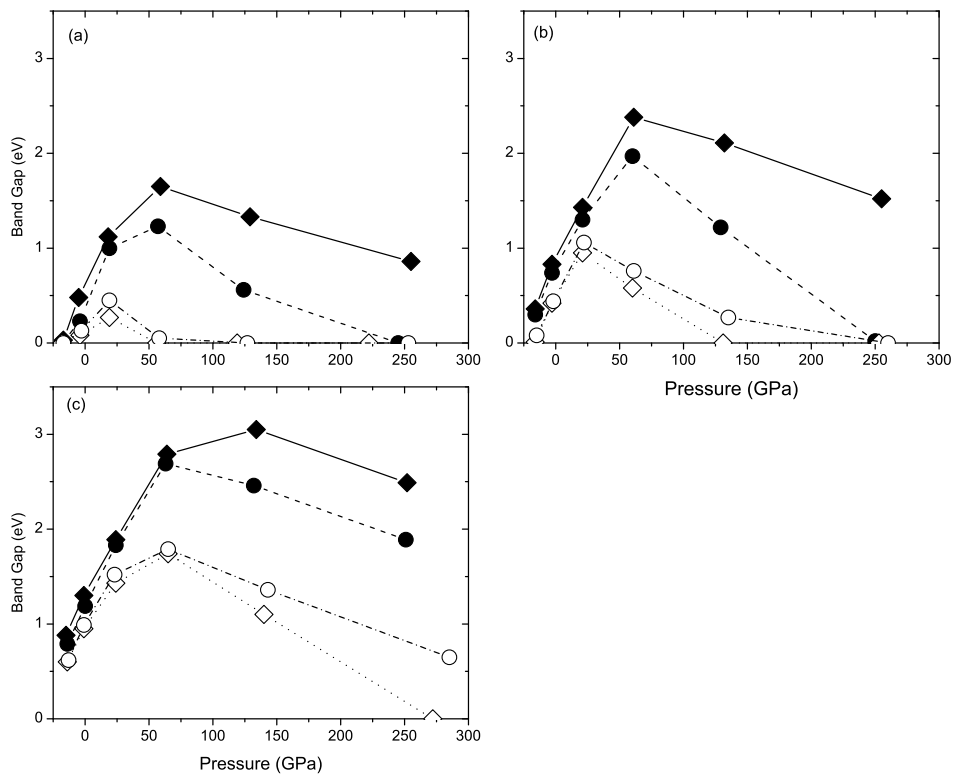


Fig. 18. – Band gaps as a function of pressure for different LDA + U solutions for FeO: (a) $U = 4.6$ eV, (b) $U = 6.0$ eV, (c) $U = 8.0$ eV. Solid symbols, rhombohedral solutions; open symbols, monoclinic solutions. Diamonds, cubic lattice; circles, rhombohedrally-strained FeO.

Keck Foundation.

REFERENCES

- [1] MCMAHAN A. K., HUSCROFT C., SCALETTAR R. T., and POLLOCK E. L., *J. Comp. Aided Mat. Design*, **5** (1998) 131
- [2] SLATER J. C., *Phys. Rev.*, **165** (1968) 165–669
- [3] COHEN R. E., STIXRUDE L., and WASSERMAN E., *Phys. Rev. B*, **56** (1997) 8575–8589
- [4] COHEN R. E., MAZIN I. I., and ISAAK D. G., *Science*, **275** (1997) 654–657
- [5] ZAAANEN G. J., SAWATZKY A., and ALLEN J. W., *Phys. Rev. Lett.*, **55** (1985) 418–421
- [6] BRANDOW B. H., *Adv. Phys.*, **26** (1977) 651–808
- [7] PERDEW J. P., BURKE K., and ERNZERHOF M., *Phys. Rev. Lett.*, **77** (1996) 3865–3868
- [8] MOTT N. F., *Metal-Insulator Transitions* (Taylor & Francis, New York) 1990.
- [9] TOWLER M. D., ALLAN N. L., HARRISON N. M., SAUNDERS V. R., MACKRODT W. C., and APRA E., *Phys. Rev. B*, **50** (1994) 5041–5054
- [10] ANISIMOV V. I., ZAAANEN J., and ANDERSEN O. K., *Phys. Rev. B*, **44** (1991) 943–954
- [11] ANISIMOV V. I., SOLOVYEV I. V., KOROTIN M. A., CZYZYK M. T., and SAWATZKY G. A., *Phys. Rev. B*, **48** (1993) 16929–16934
- [12] LIECHTENSTEIN A. I., ANISIMOV V. I., and ZAAANEN J., *Phys. Rev. B*, **52** (1995) R5467–R5470
- [13] ANISIMOV V. I., ARYASETIAWAN F., and LICHTENSTEIN A. I., *J. Phys.: Cond. Matt.*, **9** (1997) 767–808
- [14] DUDAREV S. L., BOTTON G. A., SAVRASOV S. Y., SZOTEK Z., TEMMERMAN W. M., and SUTTON A. P., *phys. stat. sol. (a)*, **166** (1998) 429–443
- [15] SINGH, D. J., *Phys. Rev. B*, **48** (1993) 14099–14103
- [16] DUDAREV S. L., PENG L. M., SAVRASOV S. Y., and ZUO J. M., *Phys. Rev. B*, **61** (2000) 2506–2512
- [17] SZOTEK Z. and TEMMERMAN W. M., *Phys. Rev. B*, **7** (1993) 4029–4032
- [18] SVANE A. and GUNNARSSON O., *Phys. Rev. Lett.*, **65** (1990) 1148–1151
- [19] BRAICOVICH L., CICCACCI F., PUPPIN E., SVANE A., and GUNNARSSON O., *Phys. Rev. B*, **46** (1992) 12165–12174
- [20] STRANGE P., SVANE A., TEMMERMAN W. M., SZOTEK Z., and WINTER H., *Nature*, **399** (1999) 756–758
- [21] GEORGES A., KOTLIAR G., KRAUTH W., and ROZENBERG M. J., *Rev. Mod. Phys.*, **68** (1996) 13–125
- [22] SAVRASOV S. Y., and G. KOTLIAR, PICTURE E. ABRAHAMS, *Nature*, **410** (2001) 793–795
- [23] BRANDOW B. H., *J. Alloys Comp.*, **181** (1992) 377–396
- [24] STIXRUDE L., COHEN R. E., and SINGH D., *Phys. Rev. B*, **50** (1994) 6442–6445
- [25] STIXRUDE L. and COHEN R. E., *Geophys. Res. Lett.*, **22** (1995) 125–128
- [26] STEINLE-NEUMANN, G., STIXRUDE L., and COHEN R. E., *Phys. Rev. B*, **60** (1999) 791–799
- [27] COHEN R. E., FEI Y., DOWNS R., MAZIN I. I., and ISAAK D. G., in *High-Pressure Materials Research*, edited by WENTZCOVITCH R., HEMLEY R. J., NELLIS W. J., and YU P. (volume 499. Materials Research Society, Pittsburgh, PA) 1998.
- [28] DRICKAMER H. G. and FRANK C. W., *Electronic Transition and the High Pressure Chemistry and Physics of Solids* (Chapman and Hall, London), 1973.
- [29] HEMLEY R. J. and MAO H.-K., *Intl. Geo. Rev.*, **32** (2001) 1–30
- [30] SINGH D. J., PICKETT W. E., and KRAKAUER H., *Phys. Rev. B*, **43** (1991) 11628–11634
- [31] WASSERMAN E., STIXRUDE L., and COHEN R. E., *Phys. Rev. B*, **53** (1996) 8296–8309
- [32] JEPHCOAT A. P., MAO H.-K., and BELL P. M., *J. Geophys. Res.* **1986**, **95** (21737)
- [33] MAO H.-K., WU Y., CHEN L. C., SHU J. F., and JEPHCOAT A. P., *J. Geophys. Res.*, **95** (1990) 21737–21742
- [34] CORT G., TAYLOR R. D., and WILLIS J. O., *J. Appl. Phys.*, **53** (1982) 2064–2065

- [35] TAYLOR R. D., PASTERNAK M. P., and JEANLOZ R., *J. Appl. Phys.*, **69** (1991) 6126–6128
- [36] NICOL M. F. and JURA G., *Science*, **141** (1963) 1035–1038
- [37] TAYLOR R. D., CORT G., and WILLIS J. O., *J. Appl. Phys.*, **53** (11)1982:8199–8201
- [38] MERKEL S., GONCHAROV A., MAO H., GILLET P., and HEMLEY R., *SCIENCE*, **288** (5471)2000:1626–1629
- [39] TSUNODA Y., *J. Phys.: Cond. Matt.*, **1** (1989) 10427–10438
- [40] GALANAKIS I., ALOUANI M., WILLS J., and DREYSSE H., *Phil. Mag. B*, **78** (5-6)1998:463–467
- [41] MEHL M. J., PAPACONSTANTOPOULOS D., MAZIN I. I., BACALIS N. C., and PICKETT W. E., *J. Appl. Phys.*, **89** (2001) 6880–6882
- [42] MRYASOV O. N., GUBANOV V. A., and LIECHTENSTEIN A. I., *Phys. Rev. B*, **45** (1992) 12330–12336
- [43] RUEFF J. P., KRISCH M., CAI Y. Q., KAPROLAT A., HANFLAND M., *et al.*, *Phys. Rev. B*, **60** (21)1999:14510–14512
- [44] SHIMIZU K., KIMURA T., FUROMOTO S., TAKEDA K., KONTANI K., *et al.*, *Nature*, **412** (2001) 316–318
- [45] PFLEIDERER C., UHLARZ M., HAYDEN S. M., VOLLMER R., LOHNEYSSEN H. V., *et al.*, *Nature*, **412** (2001) 58–61
- [46] M. R. NORMAN, *Phys. Rev. B*, **40** (1989) 10632–10634
- [47] DUFEK P., BLAHA P., and SCHWARZ K., *Phys. Rev. B*, **50** (1994) 7279–7283
- [48] ISAAK D. G., COHEN R. E., MEHL M. J., and SINGH D. J., *Phys. Rev. B*, **47** (1993) 7720–7731
- [49] SOLOVYEV I. V., LIECHTENSTEIN A. I., and TERAKURA K., *Phys. Rev. Lett.*, **80** (1998) 5758–5761
- [50] MAZIN I. I. and ANISIMOV V. I., *Phys. Rev. B*, **55** (1997) 12822–12825
- [51] VINET P., ROSE J. H., FERRANTE J., and SMITH J. R., *Phys. Cond. Matt.*, **1989** (1) 1941
- [52] FEI Y. and MAO H.-K., *Science*, **266** (1994) 1668–1680
- [53] Y. FEI, in *Mineral Spectroscopy: A Tribute to Roger G. Burns*, edited by DYAR M. D., MCCAMMON C. and SHAEFER M. W. (The Geochemical Society, Special Publication No. 5, 243–254), 1996.
- [54] MAZIN I. I., FEI Y., DOWNS J. W. and COHEN R. E., *Amer. Mineral.*, **83** (1998) 451–457
- [55] KOROTIN M. A., POSTNOKOV A. V., NEUMANN T., BORSTEL G., ANISIMOV V. I., and METHFESSEL M., *Phys. Rev. B*, **49** (1994) 6548–6552
- [56] YAGI T., SUZUKI K., and AKIMOTO S., *J. Geophys. Res.*, **90** (1985) 8784–8788
- [57] PICKETT, W. E., *J. Korean Phys. Soc.*, **1996** (29) S70
- [58] ALFE D., GILLAN M., and PRICE G., *Nature*, **401** (1999) 462–464
- [59] LAIO A., BERNARD S., CHIAROTTI G., SCANDOLO S., and TOSATTI E., *Science*, **287** (2000) 1027–1030
- [60] VOCADLO L., BRODHOLT J., ALFE D., PRICE G., and GILLAN M., *Geophys. Res. Lett.*, **26** (1999) 1231–1234
- [61] ALFE D., GILLAN M., and PRICE G., *Nature*, **405** (2000) 172–175
- [62] VOCADLO L., BRODHOLT J., ALFE D., GILLAN M., and PRICE G., *Phys. Earth Planet. Inter.*, **117** (2000) 123–137